Perpendicular Orientation of Dispersed Rubber in an Oriented Polypropylene Sheet

Panitha Phulkerd[1]*, Yoshiaki Funahashi[1], Shohei Iwasaki[2], and Masayuki Yamaguchi[1]

[1]School of Materials Science,
Japan Advanced Institute of Science and Technology
1-1 Asahidai, Nomi, Ishikawa 923-1292, JAPAN

[2] New Japan Chemical Co., Ltd.,
13 Yoshijima, Yaguracho, Fushimi, Kyoto 612-8224, JAPAN

* Corresponding author:
Panitha Phulkerd
School of Materials Science, Japan Advanced Institute of Science and Technology,
1-1 Asahidai, Nomi, Ishikawa 923-1292, Japan
Phone: +81-761-51-1623; Fax: +81-761-51-1149;
E-mail: panitha@jaist.ac.jp

Abstract

An immiscible blend of isotactic polypropylene (PP) and ethylene-butene-1 copolymer (EB) (PP/EB = 70/30) containing a small amount of *N,N'*-dicyclohexyl-2,6-naphthalenedicarboxamide as a nucleating agent for β-form crystals was prepared by T-die extrusion. We successfully prepared an extruded sheet, in which the orientation of the PP molecules is perpendicular to the deformation of the EB particles; i.e., the β-form crystals of PP are predominantly oriented perpendicular to the flow direction of the sheet plane (the transverse direction, TD), whereas the EB droplets are strongly deformed in the flow direction. It should be noted that the EB barely affects the crystalline form and orientation of PP. This extraordinary structure provides unique mechanical anisotropy. The tear strength in the TD sample is significantly enhanced with the anomalous crack propagation in the machine direction (MD). Moreover, the anisotropy in tensile properties such as Young's modulus, yield stress, strain at break, and dynamic tensile modulus becomes reduced.

Keywords: polypropylene; ethylene-butene-1 copolymer; T-die extrusion; mechanical anisotropy

Introduction

Isotactic polypropylene (PP) is widely used in various applications because it is inexpensive and lightweight. In particular, the trend in the automobile industry to use PP will continue because weight reduction is an inevitable future priority. Generally speaking, both rigidity and high impact strength are required for a material design of PP [1]. Therefore, the technology of the blend with rubber [1-17] and fillers [18,19] and the addition of a nucleating agent [20-25] has been intensively studied. Various types of elastomeric materials have been employed as impact modifiers. In particular, after the development of metallocene catalyst, ethylene-butene-1, ethylene-hexene-1, and ethylene-octene-1 copolymers have been preferred for this purpose, because they have low interfacial tension with PP compared with traditional ethylene-propylene copolymers. Such miscibility and/or compatibility have been predicted by the difference in statistical segment length [1,12,17] and packing length [8,14,17], and have been summarized from the perspective of the species and content of the α-olefin [2,3,7,15]. The rheological properties [4,5,9], crystallization behavior [6,16], and processability [10,11] of PP blends with ethylene-α-olefin copolymers have also been elucidated. Accordingly, controlling the particle size of a rubber dispersion in a PP continuous phase improves the mechanical properties of the material. In general, low interfacial tension, and viscosity matching between components enable the formation of small particles with uniform dispersion by melt blending. Furthermore, the nucleation process of PP plays a key role in the processing operation because its mechanical properties are largely dependent on the form and degree of crystallinity. As well known, PP has various crystalline forms such as monoclinic α modification, trigonal β modification, orthorhombic γ modification, and

74 smectic form, which are determined by crystallization conditions and additives
75 [2,3,7,8,12,14,17]. Of all the crystalline structures, recent attention has focused on β-form
76 crystals owing to the development of highly efficient nucleating agents such as 1,3,5-
77 benzenetrisamide [26] and *N,N'*-dicyclohexyl-2,6-naphthalenedicarboxamide [27,28].
78 These nucleating agents enhance the modulus, which was considered one of the
79 unfavorable properties of β-form crystals. Moreover, a recent report on the enhancement
80 of the melting point using β-form crystals [29] should encourage the industrial
81 applications.

82 *N,N'*-dicyclohexyl-2,6-naphthalenedicarboxamide has been used to ensure the
83 molecular orientation of the PP chains in the transverse direction (TD) [30-35]. Under
84 suitable processing conditions, the nucleating agent appears as needle-shaped crystals in
85 PP, and is aligned with the direction of flow by hydrodynamic force. Owing to the unique
86 crystallization behavior of PP, in which the *c*-axis of the PP crystals grows perpendicular
87 to the long axis of the needle-shaped nucleating agent by epitaxial crystallization, the PP
88 chains orient perpendicular to the flow direction during T-die extrusion [31]. The resulting
89 product has unique mechanical properties. Orientation control using nucleating agents is
90 applicable to injection-molding. The peculiar orientation of the PP chains, i.e., in a
91 plywood-like structure, prohibits crack propagation and reduces anisotropy in modulus
92 and in thermal expansion [32,35]. A combined approach involving the addition of rubber
93 and the control of orientation using a specific β nucleating agent is expected to maximize
94 the mechanical performance of PP. Although several papers have been published
95 regarding polymer blends of PP and ethylene-α-olefin copolymers, there have been few
96 reports describing in detail of PP blends containing a β nucleating agent [36-39].

Furthermore, in industrial applications the molecular orientation of the PP and the rubber dispersion are controlled independently.

The present research focuses on an extruded sheet comprising PP and ethylene-butene-1 copolymer (EB) with the nucleating agent, *N,N*'-dicyclohexyl-2,6-naphthalene-dicarboxamide. The orientation of the PP molecular chains and the deformation direction of the rubber particles are investigated in detail with an evaluation of the mechanical properties.

Materials and Methods

Materials

The raw materials used in the present study were: a commercially available isotactic polypropylene homopolymer (PP) (SunAllomer, PM600A, melt flow rate (MFR) 7.5 [g/10 min at 230°C], Mn 63,000, Mw 360,000), and an ethylene-butene-1 copolymer (EB) (Mitsui Chemicals, TAFER DF610, MFR 2.2 [g/10 min at 230°C], density 860 kg/m^3, ethylene content 54 wt.%). *N,N'*-dicyclohexyl-2,6-naphthalenedicarboxamide (New Japan Chemical, NJ Star NU-100) was used as a β nucleating agent without further purification.

Sample preparation

Melt-mixing of PP with 0.1 wt.% of the β nucleating agent was performed by a counter-rotating twin-screw extruder (Technovel, KZW15TW-45MG-NH) with 0.05 wt.% of 3-(3,5-di-tert-butyl-4-hydroxyphenyl)propionate (Ciba, Irganox 1010) and 0.1 wt.% of tris(2,4-di-tert-butyl-phenyl)phosphate (Ciba, Irgafos 168) as thermal stabilizers,

and 0.05 wt.% of calcium stearate (Nitto Kasei Kogyo) as a neutralizing agent. The screw diameter of the extruder was 15 mm and the length-to-diameter ratio was 45. The machine was operated at a screw rotation speed of 250 rpm. The mixing was performed at 260°C to completely dissolve the nucleating agent in molten PP. The extruded strands were dipped in a water-bath and cut into pellets approximately 2.3 mm in diameter.

The pellets of PP containing the nucleating agent and EB were fed into a single-screw extruder (Technovel, SZW25GT-28VG-STD) equipped with a T-die (300 mm wide with a 0.5 mm die lip) at a blend ratio of 70/30 (PP/EB) by weight. The out-put rate was 3 kg/h. The screw diameter and the length-to-diameter ratio were 25 mm and 28, respectively. The speed of screw rotation was 40 rpm. The sheet was stretched in the air gap (10 mm) between the die lip and the chill roll. The temperatures of the die and chill roll were maintained at 200°C and 103°C, respectively. The diameter of the chill roll was 250 mm and the rotational speed was 1 rpm. Reference samples comprising extruded sheets of PP containing the nucleating agent and PP/EB without the nucleating agent were also prepared under conditions identical to those described above.

Measurements

Thermal analysis was conducted using a differential scanning calorimeter (DSC) (Perkin Elmer, DSC 8000) under a nitrogen atmosphere to avoid thermal-oxidative degradation. Samples weighing approximately 3 mg were sealed in aluminum pans. The melting and crystallization profiles were recorded at a heating rate of 10°C min^{-1} and a cooling rate of 10°C min^{-1}.

The temperature dependence of the dynamic tensile moduli of the extruded sheets was measured between -80°C and 175°C using a dynamic mechanical analyzer

145 (UBM, Rheologel-E4000-DVE). The frequency was 10 Hz and the heating rate was 2°C
146 min^{-1}. The extruded sheet was cut into small rectangular pieces, 5 mm wide and 20 mm
147 long, that were mounted between gauges with a distance of 10 mm. The measurements
148 were carried out on two types of sample to investigate the mechanical anisotropy: one
149 was cut parallel to the flow direction (the machine direction (MD) sample), and the other
150 was perpendicular to the flow direction (the transverse direction (TD) sample). In the case
151 of the MD sample, the direction of the applied oscillatory strain coincided with the flow
152 direction.

153 To analyze the orientation and crystalline form of the PP molecules, wide-angle
154 X-ray diffraction (WAXD) patterns were collected using a high-speed two-dimensional
155 X-ray detector (Rigaku, PILATUS 3R 100K). The measurements were carried out using
156 CuKα radiation operated at 40 kV and 30 mA with a scanning range of 2θ (the Bragg
157 angle) from 10° to 30°. Small pieces of the sample (approximately 1.0 mm thick) were
158 mounted on the diffractometer. The X-ray beam was irradiated normal to the MD-ND
159 plane (edge view: EV) and the MD-TD plane (through view: TV). For the EV
160 measurements, ten sheets of the sample were laminated with polystyrene solution,
161 whereas only one sheet was used for the TV measurements.

162 The orientation of the PP lamellae was investigated using a transmission electron
163 microscopy (TEM) (JEOL, JEM-2100FX) at an acceleration voltage of 200 kV. The
164 samples were embedded in epoxy resin and sectioned using an ultramicrotome (RMC-
165 Boeckeler, Ultramicrotome MT-XL) equipped with a diamond knife after exposure to the
166 vapor of ruthenium tetraoxide at 40°C for a day. Cross-sectional specimens (100 nm
167 thick) were cut from the stained sample in the MD-ND plane.

168 The deformation of the EB dispersed phase was observed by means of a scanning
169 electron microscopy (SEM) (Hitachi, S4100) with an acceleration voltage of 20 kV. For
170 non-conductive samples, the specimens were coated with Pt/Pd alloy for 60 seconds by
171 an ion sputtering machine (Hitachi, E1010). The surface of specimen was removed using
172 a rotary microtome (Yamato Kohki Industrial, RX-860) and immersed in xylene at room
173 temperature for 3 days to elute the rubber particles.

174 Stress-strain curves were investigated at room temperature using a tensile
175 machine (Tokyo Testing Machine, LSC-05/300) following ASTM D638. The specimens
176 were cut into dumbbell-shaped pieces (10 mm wide and 40 mm long) using dumbbell
177 cutter No.3 referenced from JIS K6251, in which the sample size was reduced by 40%.
178 The initial distance between the gauges was 30 mm, and one of the crossheads was moved
179 up at a constant speed of 10 mm min^{-1}. Stretching was performed in two directions: one
180 was parallel to the flow direction (the machine direction (MD) sample) and the other was
181 perpendicular to the flow direction (the transverse direction (TD) sample). All
182 measurements were performed at least five times, and the average values were calculated.
183 The elongation at break was evaluated by measuring the final gauge length of the narrow
184 part of the dumbbell.

185 The tear test was investigated by the Trouser method using a tensile machine
186 (Tokyo Testing Machine, LSC-05/300). Two types of sample were cut from the extruded
187 sheet; one had a notch parallel to the flow direction, that is, the machine direction (MD),
188 and the other had a vertical notch, that is, the transverse direction (TD). The specimens
189 were stretched at room temperature at a speed of 200 mm min^{-1}. The distance between
190 the gauges was 20 mm.

191

Results and Discussion

Characterization of blend sheets

The melting and crystallization behaviors of the extruded sheets are shown in Fig. 1. As shown in Fig. 1a, the pure PP sheet exhibits a main melting peak at 165°C, suggesting α-form crystals with a small shoulder peak of β-form crystals at 150°C. A similar melting profile is observed in the PP/EB sheet. For the sheet containing the nucleating agent, two distinct peaks are detected at 145°C and 151°C, which can be attributed to β-form crystals. Furthermore, a sharp peak due to the α-form crystals appears at a slightly higher temperature than that for pure PP. The recrystallization after melting of thick β-form crystals is responsible for thick lamellae of α-form crystals leading to the enhanced melting point as explained by Phulkerd et al. [29]. The same phenomenon is observed for the PP/EB sheet containing the nucleating agent. Under suitable cooling conditions, an annealed sheet of PP containing the nucleating agent has a melting point due to α-form crystals nearly at 170°C [29].

The crystallization behavior during the cooling process from 200°C is shown in Fig. 1b. There is no significant difference in the exothermic crystallization temperature (ca. 117°C) between the pure PP and PP/EB sheets. After the addition of the nucleating agent, the crystallization peak shifts to a higher temperature at 128°C in both the PP and PP/EB sheets. In this experiment, the crystallization temperature of PP is barely affected by EB irrespective of the addition of the nucleating agent, which also indicates that EB particles hardly affect the nucleating ability of the nucleating agent.

[Fig. 1]

Fig. 2 shows the X-ray diffraction curves in the equatorial direction of the MD-TD plane, which are transformed and corrected using Lorentz and polarization (Lp) factors. Both α- and β-form crystals are detected but the β-form crystals are predominant in the sheets containing the nucleating agent. In the sheets without the nucleating agent, the strong peak ascribed to the α-form crystals are detected, although β(110) and β(111) peaks are still confirmed. Relatively high cooling temperature (the chill roll was maintained at 103°C) induces the β-form crystallization to some extent. The XRD patterns also suggest that the addition of EB to PP has a negligible effect on crystal formation. Furthermore, there is an indication that the crystallinity of EB is significantly low in the extruded sheets, because both (110) and (200) planes, which are attributable to polyethylene crystals, are absent.

[Fig. 2]

Fig. 3 shows the 2D-WAXD patterns of the extruded sheets, obtained by directing the X-ray beam in the normal direction for the edge view and in the transverse direction for the through view. The α-form crystals in the pure PP show weak orientation, as seen in Fig. 3a. The diffraction patterns of the PP/EB sheet (Fig. 3b) are almost identical to those of the PP sheet, in which a diffraction peak attributed to the (040) plane of the α-form crystals is detected in the equatorial direction, demonstrating that the PP molecular chains are oriented in the MD direction. For the PP sheet containing the nucleating agent (Fig. 3c), the PP chains in the β-form crystals were oriented in the TD direction. Such molecular orientation is also detected in the PP/EB sheet containing the nucleating agent, in which distinct arcs ascribed to (110) reflection of the β-form crystals

240 are observed as shown in Fig. 3d. This result demonstrates that PP chains preferentially
241 orient perpendicular to the flow direction. It also indicates that the nucleating agent
242 promotes the growth of β-form crystals with the TD orientation of the PP molecular chains,
243 irrespective of the presence of EB.
244
245 [Fig. 3]
246
247 Fig. 4 shows a TEM image of a thin slice of the TD-ND plane cut from the PP/EB
248 sheet containing the nucleating agent. Phase-separated morphology is clearly seen in this
249 sample, in which the dark region is the EB phase. Furthermore, the crystalline lamellae
250 of PP are detected in the matrix as white lines, which preferentially orient along the ND.
251 Therefore, the growth direction of the PP chains is perpendicular to the ND, i.e., the TD
252 orientation, which corresponds well with the XRD patterns. The compressed stress
253 applied during the chill roll process is responsible for the preferential TD orientation of
254 PP chains, not the ND orientation. The slight deformation of EB particles to the TD would
255 be also attributed to the compression stress at the chill roll, although the deformation of
256 EB particles will be explained in detail later. Furthermore, PP lamellae are incorporated
257 into EB phase, which will provide the strong adhesion between them. This phenomenon
258 is attributed to the low interfacial tension between PP and EB, leading to large interphase
259 thickness in the molten state.
260
261 [Fig. 4]
262
263 Fig. 5 shows SEM images for the PP/EB sheet containing the nucleating agent.

The dark regions are attributable to the elongated pores formed by elution of the EB particles with xylene. As seen in Fig. 5a, the numerous pores are mainly deformed in the flow direction. The length of the pores is found to be approximately 3.0 μm and the diameter is about 0.5 μm. On the other hand, a slight deformation in the TD direction with an averaged pore size of 1.0 μm for the length and 0.5 μm for the diameter is detected in the TD-ND plane, owing to the pressure applied by the chill roll, which corresponds with the TEM image. The marked difference in the pore size between the MD and TD directions demonstrates that EB preferentially orients in the flow direction. This is understandable because the elongational stress in the air gap as well as the shear stress in the die deform the EB particles in the flow direction by the hydrodynamic force. Similar SEM images were obtained for the PP/EB sheet without the nucleating agent (but they are not presented here). This suggests that the nucleating agent hardly affects the rubber dispersion and deformation.

[Fig. 5]

Mechanical properties

Because the molecular orientation of PP is different from that of EB, the sample sheet exhibits anomalous mechanical properties. Fig. 6 shows the dynamic mechanical properties of extruded sheets employing two specimens to apply the oscillatory stain in the different directions, i.e., the machine direction (MD) and transverse direction (TD). As seen in Fig. 6a, both the MD and TD samples for the pure PP sheet show almost the same dynamic tensile moduli over the whole range of temperature. A similar behavior is also detected in the PP/EB sheet, in which PP molecules orient to the flow direction. Since

288 the molecular orientation is weak, no obvious mechanical anisotropy is observed for the
289 sample sheets without the nucleating agent. Moreover, *E'* in PP/EB falls off markedly
290 around 165°C which is attributed to melting of α-form crystals. For the PP sheet
291 containing the nucleating agent, in contrast, *E'* in TD is higher than that in MD at low
292 temperatures and vice versa at high temperatures. Based on the mechanical model
293 proposed by Takayanagi et al. [40], the anisotropy of the tie chain fractions, which are
294 deformed in the flow direction by hydrodynamic force during extrusion, is responsible
295 for the crossing behavior in the sample containing the nucleating agent [33]. A similar
296 mechanical behavior is detected for the PP/EB sheet containing the nucleating agent,
297 albeit the crossing behavior is weaker and shifted to the lower temperature region. As
298 compared with the PP/EB sheet, the addition of the nucleating agent enhances *E'* for the
299 MD sample over a wide temperature range above the glass transition (T_g), owing to a high
300 degree of crystallinity resulting from the nucleating effect. Furthermore, a sharp drop of
301 *E'* is detected around 150°C due to the melting of the β-form crystals, which corresponds
302 to the DSC and WAXD results. It is found from Fig. 6b that both the PP/EB sheets with
303 or without the nucleating agent exhibit double peaks in the *E''* curve in the temperature
304 range from -75°C to 40°C; the peak at the higher temperature is attributed to T_g of PP and
305 the other at the lower one is to that of EB.
306
307 [Fig. 6]
308
309 The stress-strain curves at the strain rate of 0.006 s^{-1} are shown in Fig. 7. The
310 tensile force is applied along the MD or the TD. The difference in the tensile behavior
311 between stretching in the MD and TD is detected in all samples. As seen in Fig. 7a, the

312 pure PP sheet experiences a brittle fracture in the TD stretching beyond the yield point.
313 In the case of MD stretching, however, ductile deformation occurs under a low yield
314 stress. The PP containing the nucleating agent (Fig. 7b) shows high Young's modulus,
315 which corresponds to the tensile storage modulus. Moreover, yield stress in the MD
316 stretching is greatly enhanced with a ductile manner. The low modulus of EB is
317 responsible for marked decrease in Young's modulus and yield stress for both the PP/EB
318 and PP/EB containing the nucleating agent as seen in Figs. 7c and 7d. In the PP/EB sheet
319 containing the nucleating agent, the anisotropy in Young's modulus and yield stress is
320 considerably weaker than that in the PP sheet containing the nucleating agent. The strain
321 at break in the TD stretching for PP containing the nucleating agent is considerably larger
322 than that for pure PP. The ductile behavior is also observed in MD stretching, although
323 the yield stress is high. As a result, the anisotropy of strain at break becomes reduced
324 following the addition of the nucleating agent. The reduction of the mechanical anisotropy
325 becomes more apparent for the blend containing EB, although it is interesting to note that
326 the PP/EB exhibits ductile behavior not only in MD but also in TD stretching. Since the
327 yield stress in TD stretching is lower than that in MD stretching, the deformation of EB
328 particles into flow direction affects the stress-strain behavior greatly, although the
329 deformation behavior of the EB phase is not revealed in this study. The details of
330 mechanical anisotropy in terms of crack propagation are discussed below.
331
332 [Fig. 7]
333
334 Trouser tear test was carried out at room temperature employing two types of the
335 sheet samples; one has a parallel notch in the flow direction (MD), and the other has a

336 vertical notch (TD). As seen in Fig. 8a, the pure PP sheet shows higher tear strength in
337 the TD sample. For PP containing the nucleating agent (Fig. 8b), the order is opposite
338 with an enhanced anisotropy in tear strength. In the case of the blend, the tear strength in
339 the TD sample is markedly enhanced, irrespective of the nucleating agent. Furthermore,
340 the direction of crack propagation changes to the MD immediately after the stretching as
341 demonstrated in Figs. 8c and 8d. These results demonstrate that PP orientation has no
342 marked impact on the tear property. The deformation of EB particles plays a dominant
343 role on the tearing. Such information has never been reported before to the best of our
344 knowledge, because the deformation direction of a dispersion is always the same as the
345 molecular orientation direction of matrix in general. Regarding the effect of the nucleating
346 agent, the tear strength of the MD sample is slightly enhanced, although the effect is not
347 as obvious as in the pure PP.
348
349 [Fig. 8]
350
351
352 **Conclusions**
353
354 An extruded sheet with unique structure was developed using a blend comprising
355 PP, EB, and a small amount of *N,N'*-dicyclohexyl-2,6-naphthalenedicarboxamide. It was
356 found that the nucleating agent promotes the formation of β-form crystals and causes the
357 PP chains orient perpendicular to the flow direction in an extruded sheet, i.e., in the
358 transverse direction, as confirmed by 2D-XRD and TEM characterization. On the contrary,
359 EB is deformed in the flow direction, as revealed by SEM images. As a result, the chain

orientation of the PP molecules is perpendicular to the deformation direction of the EB droplets, which affects the mechanical anisotropy to a great extent. With regard to the tensile properties, the anisotropy in yield stress and strain at break is significantly decreased owing to this peculiar structure. It is proved by the tear test that the strength of the TD sample is increased with a crack growth in the flow direction. This result demonstrates that the deformation of the EB particles in the MD direction exhibits more pronounced effect than the molecular orientation of the PP chains in the TD direction.

References

1. F.S. Bates, G.H. Fredrickson, Conformational asymmetry and polymer-polymer thermodynamics, Macromolecules 27 (1994) 1065-1067.
2. M. Yamaguchi, H. Miyata, K-H Nitta, Compatibility of binary blends of polypropylene with ethylene-α-olefin copolymer, J. Appl. Polym. Sci. 62 (1996) 87-97.
3. P.A. Weimann, T.D. Jones, M.A. Hillmyer, F.S. Bates, J.D. Londono, Y. Melnichenko, G.D. Wignall, K. Almdal, Phase behavior of isotactic polypropylene-poly(ethylene/ethylethylene) random copolymer blends, Macromolecules 30 (1997) 3650-3657.
4. C.J. Carriere, H.C. Silvis, The effects of short-chain branching and comonomer type on the interfacial tension of polypropylene-polyolefin elastomer blends, J. Appl. Polym. Sci. 66 (1997) 1175-1181.

382 5. M. Yamaguchi, K-H Nitta, H. Miyata, T. Masuda, Rheological properties for binary
383 blends of i-PP and ethylene-1-hexene copolymer, J. Appl. Polym. Sci. 63 (1997) 467-
384 474.
385 6. M. Yamaguchi, H. Miyata, K-H Nitta, Structure and properties for binary blends of
386 isotactic polypropylene with ethylene-α-olefin copolymer. 1. Crystallization and
387 morphology, J. Polym. Sci. B Polym. Phys. 35 (1997) 953-961.
388 7. Y. Thomann, J. Suhm, R. Thomann, G. Bar, R.D. Maier, R. Mülhaupt, Investigation of
389 morphologies of one- and two-phase blends of isotactic poly(propene) with random
390 poly(ethene-co-1-butene), Macromolecules 31 (1998) 5441-5449.
391 8. D.J. Lohse, W.W. Graessley, Thermodynamics of polyolefin blends, in: D.R. Paul,
392 C.B. Bucknall (Eds.), Polymer Blends, John Wiley & Sons Inc., New York, 1999, pp.
393 219-237.
394 9. M. Yamaguchi, H. Miyata, Influence of stereoregularity of polypropylene on
395 miscibility with ethylene-1-hexene copolymer, Macromolecules 32 (1999) 5911-5916.
396 10. M. Yamaguchi, K-I Suzuki, H. Miyata, Structure and mechanical properties for binary
397 blends of polypropylene and ethylene-1-hexene copolymer, J. Polym. Sci. B Polym.
398 Phys. 37 (1999) 701-713.
399 11. E.L. Bedia, S. Murakami, K. Senoo, S. Kohjiya, Polymer 43 (2002) 749-755.
400 12. T.D. Jones, K.A. Chaffin, F.S. Bates, Effect of tacticity on coil dimensions and
401 thermodynamic properties of polypropylene, Macromolecules 35 (2002) 5061-5068.
402 13. N. Pasquini, Polypropylene Handbook, second ed., Hanser, Munich, 2005.
403 14. D.J. Lohse, The Influence of chemical structure on polyolefin melt rheology and
404 miscibility, J. Macromol. Sci. Polymer. Rev. 45 (2005) 289-308.

15. M. Yamaguchi, Morphology and mechanical properties in iPP/polyolefin-based copolymer blends, in: D. Nwabunma, T. Kyu (Eds.), Polyolefin Blends, John Wiley & Sons Inc., New Jersey, 2008, pp. 224-268.
16. J. Yang, J.L. White, Crystallization behavior of polypropylene/ethylene butene copolymer blends, J. Appl. Polym. Sci. 126 (2012) 2049-2058.
17. J. Xu, V. Mittal, F.S. Bates, Toughened isotactic polypropylene: Phase behavior and mechanical properties of blends with strategically designed random copolymer modifiers, Macromolecules 49 (2016) 6497-6506.
18. Y. Lin, H. Chen, C-M Chan, J. Wu, High impact toughness polypropylene/$CaCO_3$ nanocomposites and the toughening mechanism, Macromolecules 41 (2008) 9204-9213.
19. R. Wiwattananukul, B. Fan, M. Yamaguchi, Improvement of rigidity for rubber-toughened polypropylene via localization of carbon nanotubes, Comp. Sci. Technol. 141 (2017) 106-112.
20. Y. Feng, X. Jin, J.N. Hay, Effect of nucleating agent addition on crystallization of isotactic polypropylene, J. Appl. Polym. Sci. 69 (1998) 2089-2095.
21. J. Varga, I. Mudra, G.W. Ehrenstein, Highly active thermally stable β-nucleating agents for isotactic polypropylene, J. Appl. Polym. Sci. 74 (1999) 2357-2368.
22. G-S Jang, W-J Cho, C-S Ha, Crystallization behavior of polypropylene with or without sodium benzoate as a nucleating agent, J. Polym. Sci. B Polym. Phys. 39 (2001) 1001-1016.
23. C. Marco, M.A. Gomez, G. Ellis, J.M. Arribas, Activity of a β-nucleating agent for isotactic polypropylene and its influence on polymorphic transitions, J. Appl. Polym. Sci. 86 (2002) 531-539.

429 24. P-W Zhu, J. Tung, A. Phillips, G. Edward, Morphological development of oriented
430 isotactic polypropylene in the presence of a nucleating agent, Macromolecules 39
431 (2006) 1821-1831.
432 25. M. Liu, B. Guo, M. Du, F. Chen, D. Jia, Halloysite nanotubes as a novel β-nucleating
433 agent for isotactic polypropylene, Polymer 50 (2009) 3022-3030.
434 26. M. Kerscha, H.W. Schmidtb, V. Altstädta, Influence of different beta-nucleating agents
435 on the morphology of isotactic polypropylene and their toughening effectiveness,
436 Polymer 98 (2016) 320-326.
437 27. A. Romankiewicz, T. Sterzynski, W. Brostow, Structural characterization of α- and β-
438 nucleated isotactic polypropylene, Polym. Int. 53 (2004) 2086-2091.
439 28. Y.F. Zhang, X.X. Luo, L. Zhu, X.J. Yang, Y. Chang, Effects of α/β compound nucleating
440 agents on mechanical properties and crystallization behaviors of isotactic
441 polypropylene, J. Macromol. Sci. B. 51 (2012) 2352-2360.
442 29. P. Phulkerd, S. Arayachukeat, T. Huang, T. Inoue, S. Nobukawa, M. Yamaguchi,
443 Melting point elevation of isotactic polypropylene, J. Macromol. Sci. B. 53 (2014)
444 1222-1230.
445 30. Y. Uchiyama, S. Iwasaki, C. Ueoka, T. Fukui, K. Okamoto, M. Yamaguchi, Molecular
446 orientation and mechanical anisotropy of polypropylene sheet containing *N,N'*-
447 dicyclohexyl-2,6-naphthalenedicarboxamide, J. Polym. Sci. B Polym. Phys. 47 (2009)
448 424-433.
449 31. M. Yamaguchi, T. Fukui, K. Okamoto, S. Sasaki, Y. Uchiyama, C. Ueoka, Anomalous
450 molecular orientation of isotactic polypropylene sheet containing *N,N'*-dicyclohexyl
451 2,6-naphthalenedicarboxamide, Polymer 50 (2009) 1497-1504.
452 32. M. Yamaguchi, Y. Irie, P. Phulkerd, H. Hagihara, S. Hirayama, S. Sasaki, Plywood-like

453 structure of injection-moulded polypropylene, Polymer 51 (2010) 5983-5989.
454 33. P. Phulkerd, S. Nobukawa, Y. Uchiyama, M. Yamaguchi, Anomalous mechanical
455 anisotropy of β form polypropylene sheet with *N,N'*-dicyclohexyl-2,6-naphthalene-
456 dicarboxamide, Polymer 52 (2011) 4867-4872.
457 34. P. Phulkerd, H. Hagihara, S. Nobukawa, Y. Uchiyama, M. Yamaguchi, Plastic
458 deformation behavior of polypropylene sheet with transversal orientation, J. Polym.
459 Sci. B Polym. Phys. 51 (2013) 897-906.
460 35. P. Phulkerd, S. Hirayama, S. Nobukawa, T. Inoue, M. Yamaguchi, Structure and
461 mechanical anisotropy of injection-molded polypropylene with a plywood structure,
462 Polym. J. 46 (2014) 226-233.
463 36. J. Varga, I. Mudra, G.W. Ehrensten, Highly active thermally stable β-nucleating agents
464 for isotactic polypropylene, J. Appl. Polym. Sci. 74 (1999) 2357-2368.
465 37. C. Grein, M. Gahleitner, On the influence of nucleation on the toughness of iPP/EPR
466 blends with different rubber molecular architectures, Express. Polym. Lett. 2 (2008)
467 392-397.
468 38. Y. Chen, S. Yang, H. Yang, M. Zhang, Q. Zhang, Z. Li, Toughness reinforcement in
469 carbon nanotube-filled high impact polypropylene copolymer with β-nucleating
470 agent, Ind. Eng. Chem. Res. 55 (2016) 8733-8742.
471 39. S. Sato, T. Maeda, M. Yamaguchi, Control of chain orientation in blends of
472 polypropylene and polybutene-1, Macromol. Mater. Eng. 302 (2017) 1600413-
473 1600421.
474 40. M. Takayanagi, K. Imada, T. Kajiyama, Mechanical properties and fine structure of
475 drawn polymers, J. Polym. Sci., Part C 15 (1967) 263-281.
476

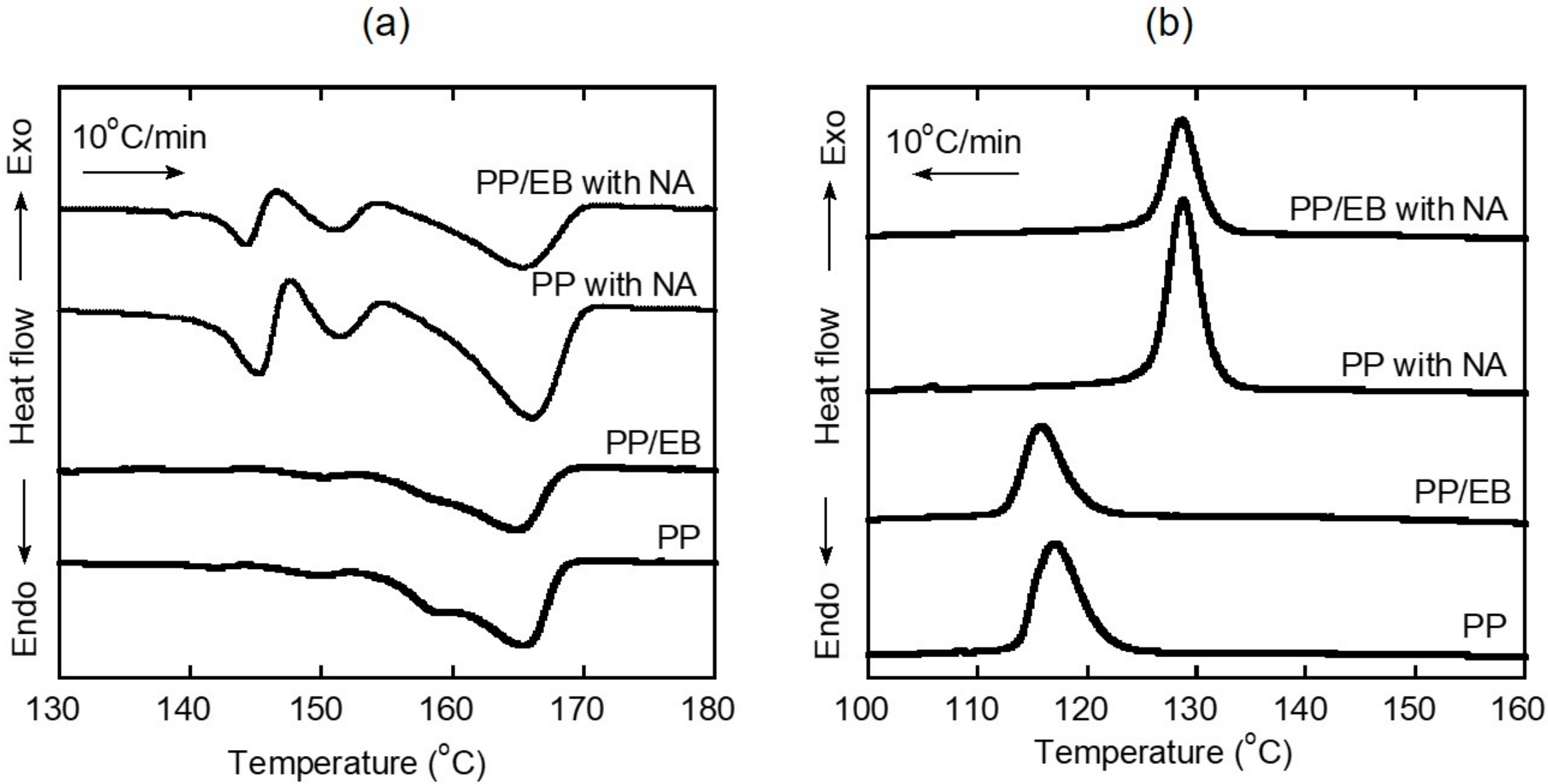

Fig. 1 DSC profiles of extruded sheets; (a) heating curves and (b) cooling curves.

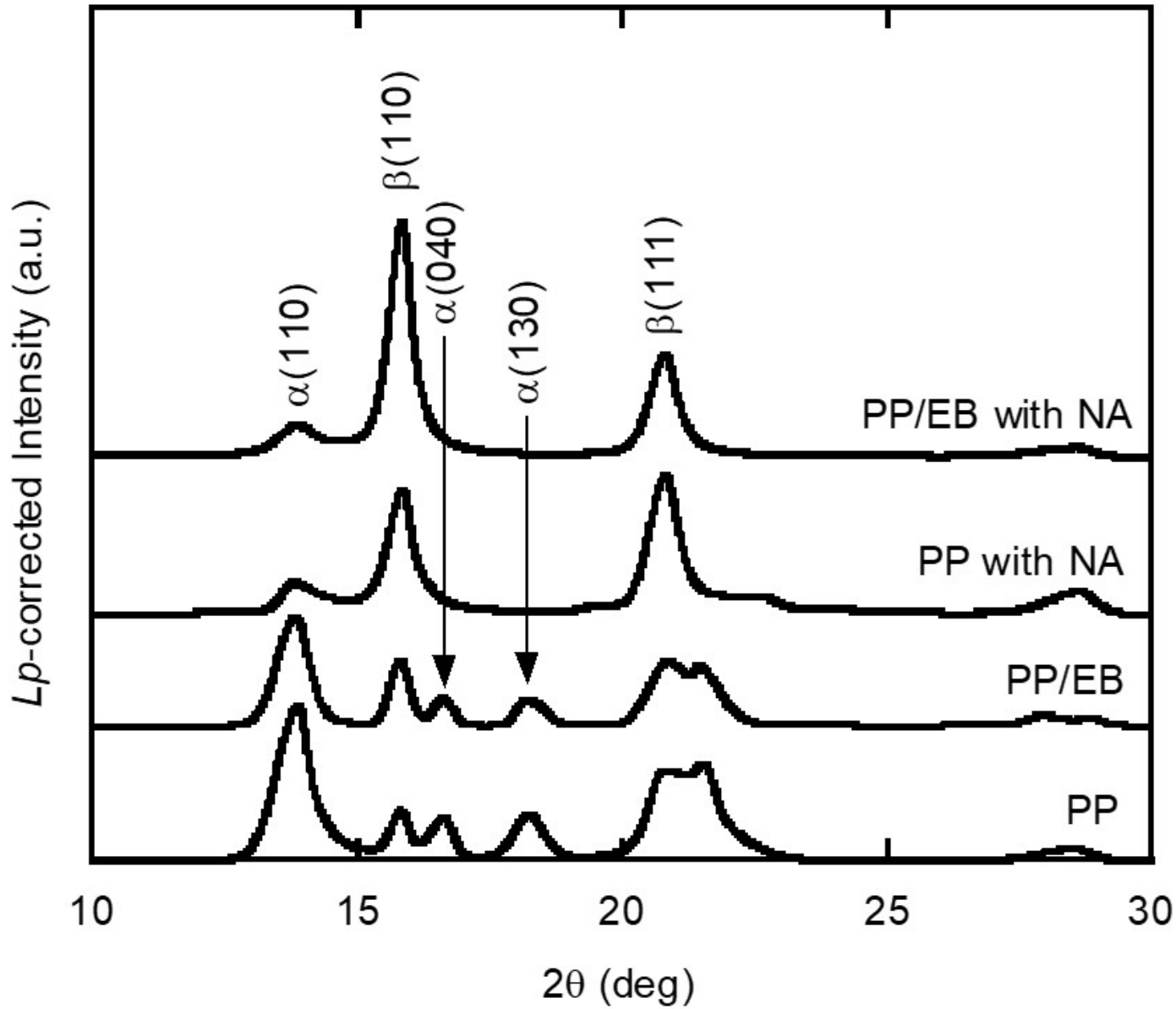

Fig. 2 Lp-corrected XRD curves obtained from the through view beam for extruded sheets.

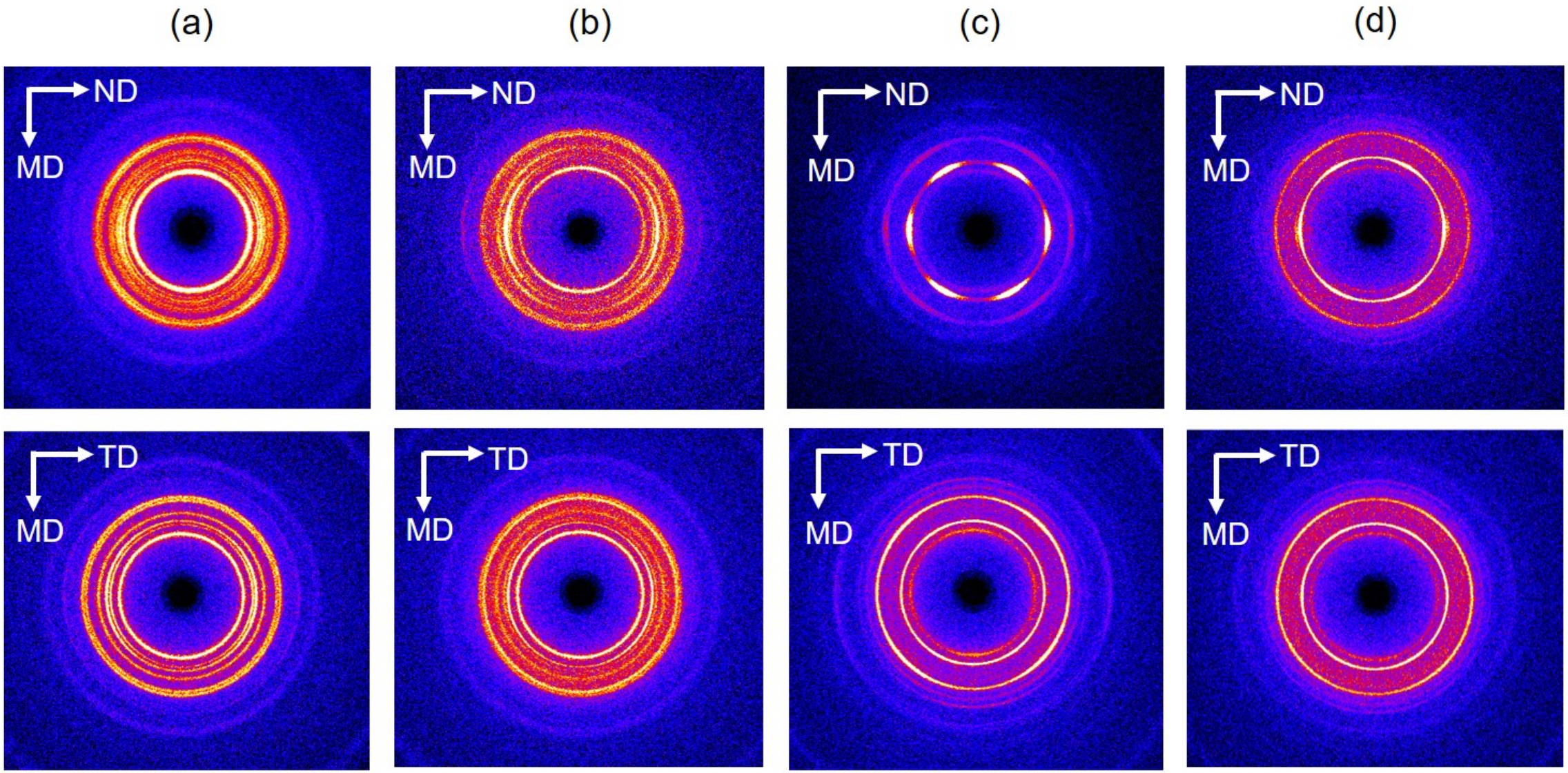

Fig. 3 WAXD patterns of the edge views (MD-ND) and the through views (MD-TD) in the samples; (a) PP, (b) PP/EB, (c) PP containing the nucleating agent, and (d) PP/EB containing the nucleating agent.

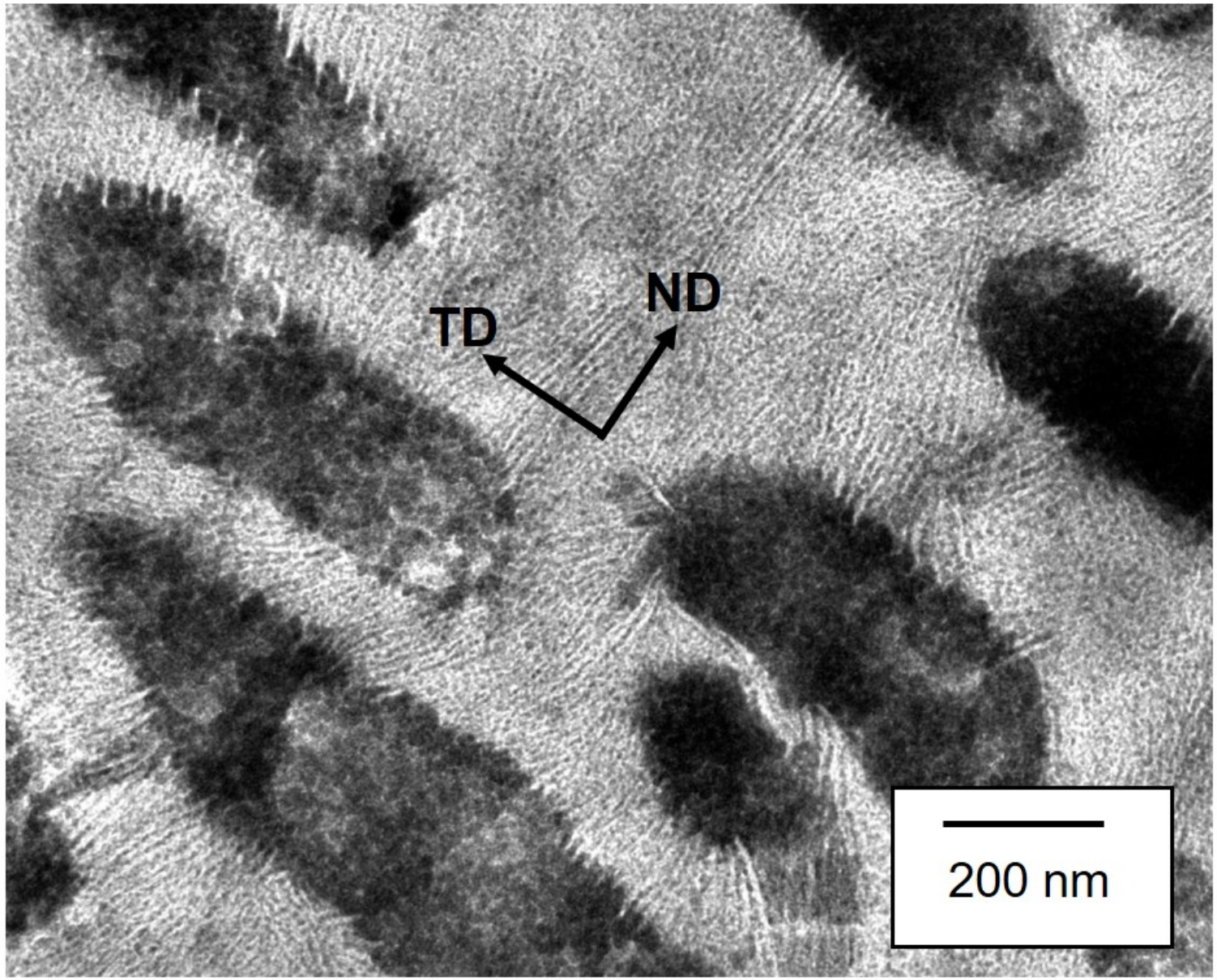

Fig. 4 TEM image of the TD-ND plane (×15,000) for PP/EB containing the nucleating agent.

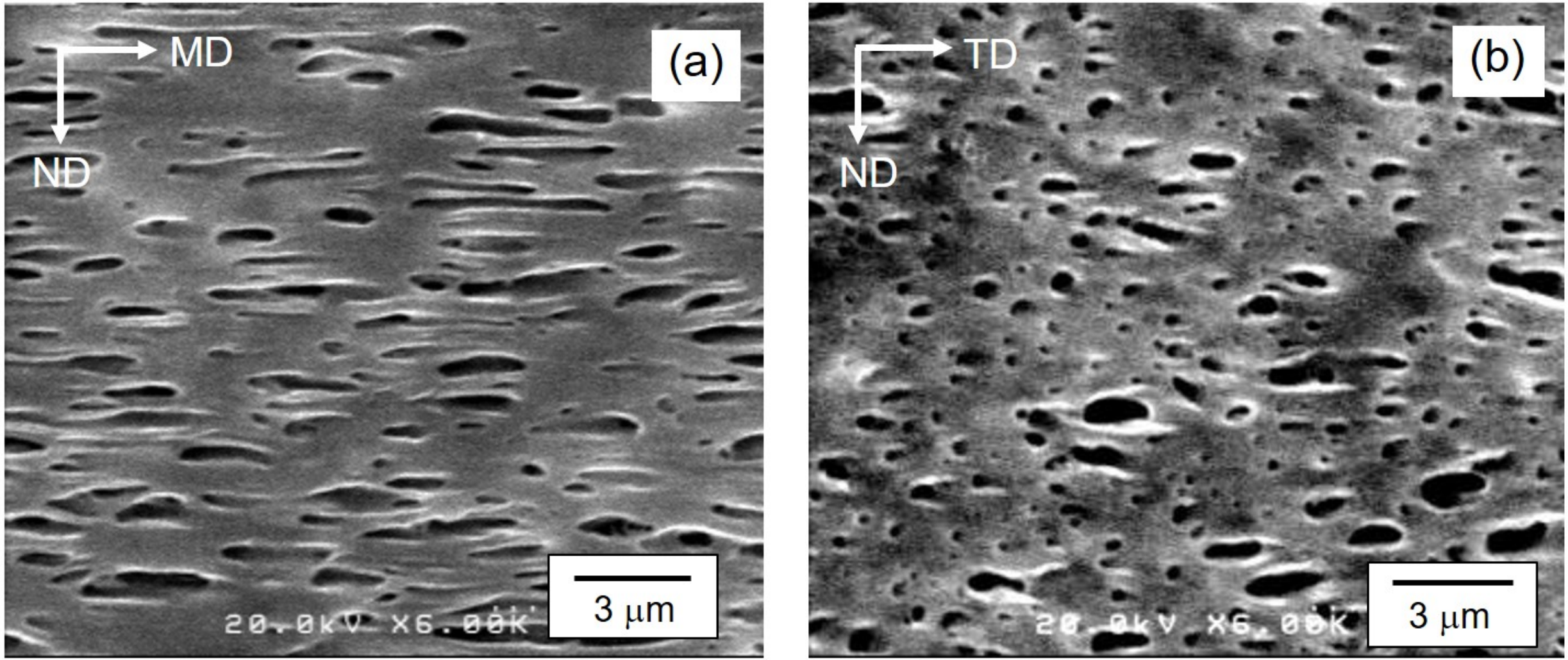

Fig. 5 SEM images of PP/EB containing the nucleating agent. (a) MD-ND plane and (b) TD-ND plane.

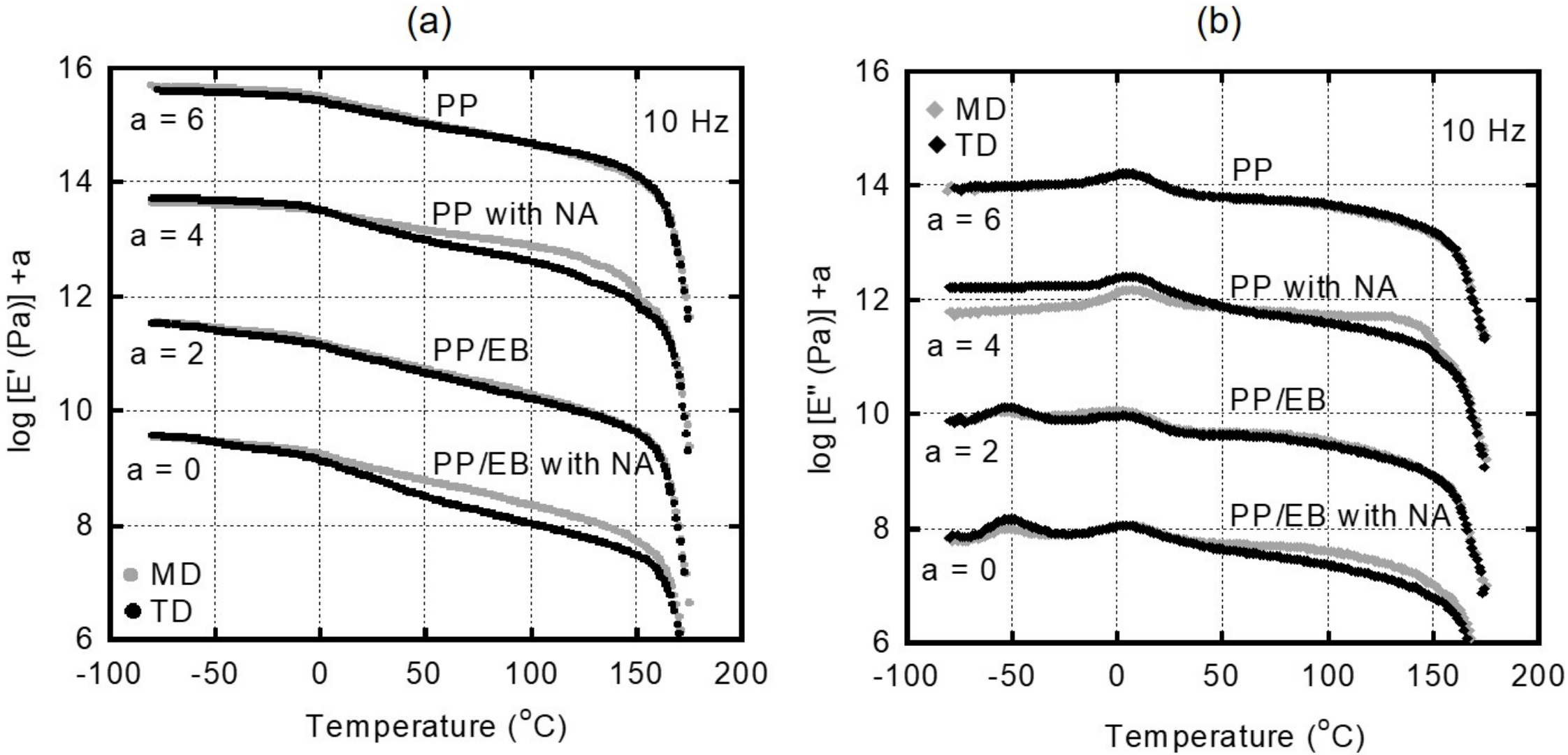

Fig. 6 Temperature dependence of dynamic tensile modulus of extruded sheets at 10 Hz; (a) tensile storage modulus *E'* and (b) tensile loss modulus *E"*. The applied strain was (grey symbol) parallel to the flow direction (MD) and (black symbol) perpendicular to the flow direction (TD).

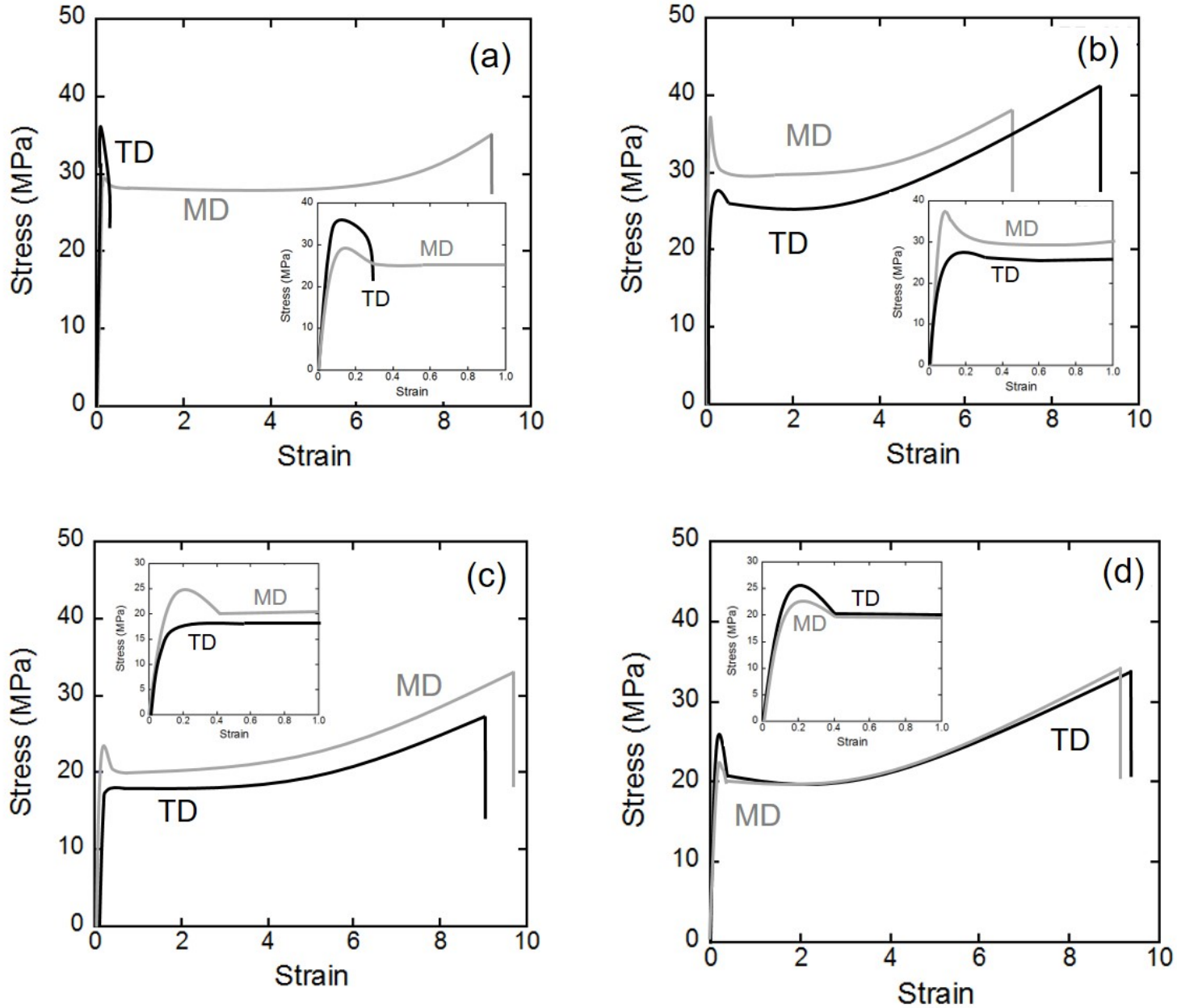

Fig. 7 Stress-strain curves of (a) PP, (b) PP containing the nucleating agent, (c) PP/EB, and (d) PP/EB containing the nucleating agent at a strain rate of 0.006 s^{-1}.

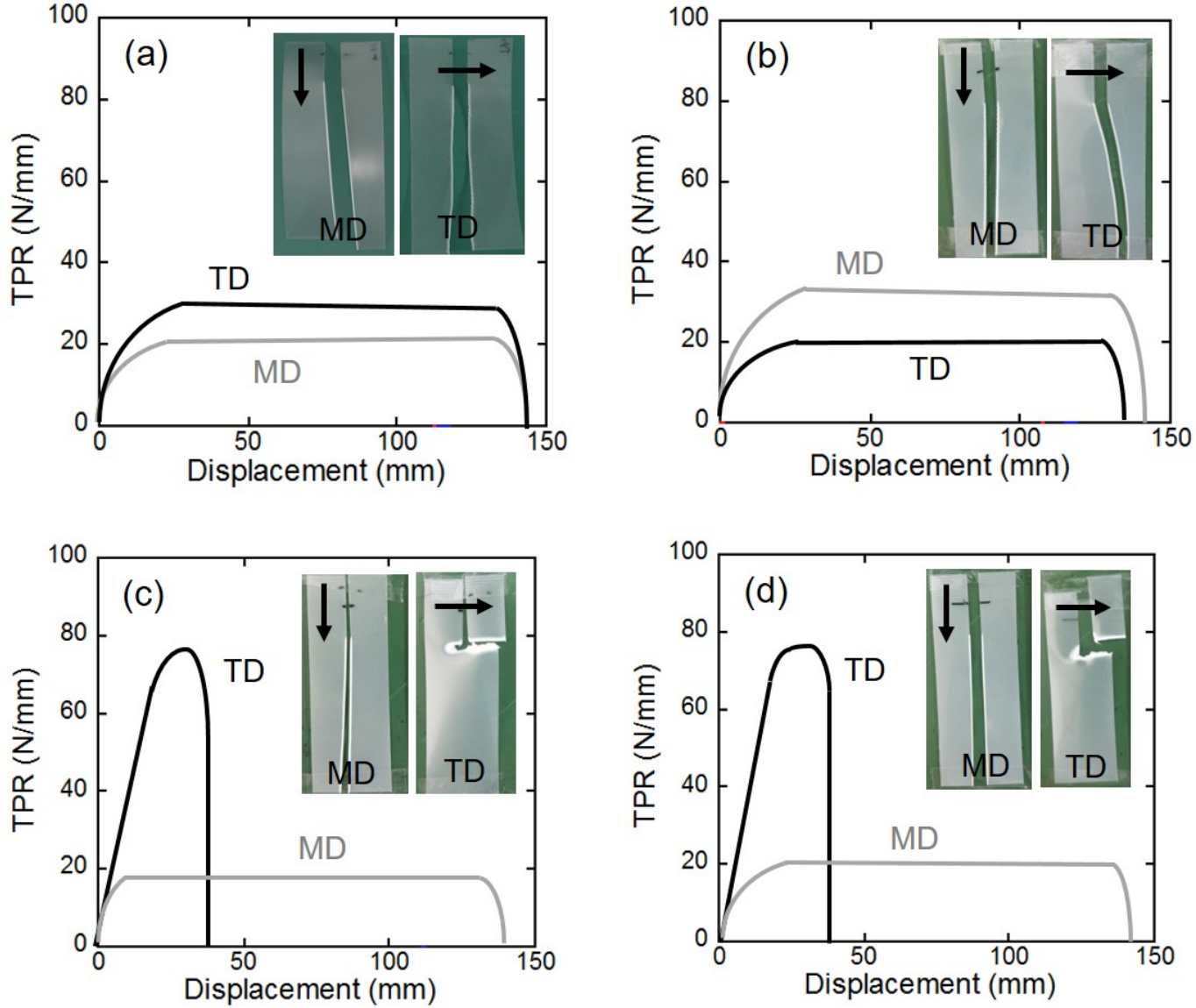

Fig. 8 Tear-propagation resistance (TPR) versus the applied displacement of notched specimens in MD and TD directions; (a) PP, (b) PP containing the nucleating agent, (c) PP/EB, and (d) PP/EB containing the nucleating agent.